

BELOW-BAND SIGNAL PROCESSING FOR LOCALIZING DISTANT SOURCES IN A NOISY DEEP OCEAN

David J. Geroski^a, David R. Dowling^b

^aDavid J. Geroski (ATTN: Alesha Thomas)

Applied Physics Program

1301 Beal Avenue

Ann Arbor MI, 48109

^bDavid R. Dowling

Department of Mechanical Engineering

1231 Beal Avenue

Ann Arbor, MI 48109

Abstract: *Frequency Difference Source Localization (FDSL) methods have proven successful for localizing sources both in the deep ocean and in the shallow ocean using recordings from a vertical array of hydrophones. These source localization algorithms are based upon the phase coherence of a product of recorded complex field values, termed autoproductions, at frequencies below the recordings' bandwidth. Similar to Matched Field Processing (MFP), the measured autoproduction is correlated to a replica that is calculated based on the user's knowledge of the acoustic environment. These below-band source localization methods are nonlinear and sacrifice in-band spatial resolution for robustness to environmental mismatch. Past frequency-difference localization efforts utilized high signal-to-noise ratio (SNR) data to demonstrate robustness to mismatch. This paper explores the performance of FDSL in the presence of noise. Specifically, simulated noise and noise measured during the PhilSea10 experiment are added to both simulated and measured pings to determine the SNR below which localization performance begins to degrade. For the scenario considered here, the source was located 210 km from a vertical receiving array in a deep ocean environment with an active internal wave field. The source broadcast was a linear frequency sweep from 200 to 300 Hz. At high SNR (>20 dB) using single-digit-Hertz below-band frequencies, the source is correctly localized in all simulations, and in 97 out of 100 trials using single-broadcast ocean recordings. For simulated and measured forward signals distorted by simulated noise, this performance persists down to SNR's of -20 and -14 dB, respectively. For measured forward signals with elevated levels of measured noise, successful performance persists down to -8 dB SNR.*

Keywords: *Source Localization, Nonlinear Signal Processing, Matched Field Processing*

1. INTRODUCTION

Passive acoustic localization of a distant unknown source is a common task in acoustic remote sensing in the ocean using hydrophone arrays (see Dowling and Sabra, 2015). One popular class of frequency-domain techniques for this task is Matched Field Processing, (MFP) which involves correlating measured fields with replica fields calculated using the known propagation physics of the acoustic environment (Bucker, 1976). MFP techniques have proven to be robust to many kinds of ocean noise (Debever and Kuperman 2007), and they work well when the acoustic environment between the source and receiving array is well known. However, a lack of sufficiently-complete environmental knowledge causes MFP to struggle in many scenarios of interest (Baggeroer et. al. 1993). This problem, known as *mismatch*, becomes more severe at higher frequencies and longer ranges, as the acoustic propagation becomes more sensitive to smaller environmental details at higher frequency, and includes larger regions of the imperfectly-known ocean environment at longer range.

Recently, this limitation has been mitigated in the shallow ocean using Frequency Difference MFP (FDMFP) to localize sources operating at high ($f > 10$ kHz) frequencies in a 103 m deep sound speed channel (Worthmann 2015, 2017). This technique involves constructing quadratic products of the measured signals and correlating them to lower frequency fields, where mismatch is less problematic. This article has two purposes: to introduce a mild revision of FDMFP, termed Frequency Difference Source Localization (FDSL), that allows distant acoustic sources to be localized in the deep ocean, and to test the noise rejection capabilities of FDSL. This performance is assessed with propagation data measured during the PhilSea10 experiment (Worcester et. al. 2013). In particular, this study focuses on localizing a single source, positioned 210 km downrange from a vertical array of transducers, that transmitted a frequency sweep signal ($200 < f < 300$ Hz) repeatedly over the course of several months. The results show that FDSL can be used to overcome mismatch in the deep ocean even at relatively low signal-to-noise ratios (SNRs).

The remainder of this paper is divided into three sections. Section 2 contains a summary of conventional MFP and FDSL, as well as descriptions of the signal processing techniques undertaken to produce the given results. Section 3 provides a brief description of the PhilSea10 experiment, the post processing used to artificially degrade the SNR achieved during the experiment, and the simulated and measured results of FDSL in this ocean environment. Section 4 summarizes this study, and states the conclusions drawn from it.

2. THEORY

The FDSL technique can be thought of as a variant of conventional MFP for array recorded acoustic signals. Given this, the most natural place to begin a discussion of this algorithm is with conventional, or Bartlett MFP (see Jensen et. al. 2011). Bartlett MFP is a spatial filtering process applied over a receiving array. Acoustic signals measured along the array from a source located at x_s , denoted in the frequency domain as $P_j(\omega)$ at angular frequency ω and for hydrophone j , are cross correlated with a weight vector $w_j(x_t, \omega)$ that represents the acoustic response of the (known) acoustic environment to a time-harmonic source transmitting from trial location x_t to hydrophone j . The trial-source location, x_t , is then varied over the region of interest to produce an ambiguity surface defined in (1).

$$B_c(x_t, \omega) = \sum_{i,j} w_i(x_t, \omega) R_{ij}(\omega) w_j^*(x_t, \omega) \quad (1)$$

$$R_{ij}(\omega) = \frac{P_i^*(\omega)P_j(\omega)}{\sum_i |P_i(\omega)|^2} \quad (2)$$

$$w_j(x_t, \omega) = G(\omega, x_t, x_j) (\sum_i |G(\omega, x_t, x_i)|^2)^{-\frac{1}{2}} \quad (3)$$

Here, $R_{ij}(\omega)$ in (2) is conventionally referred to as the cross-spectral density matrix (CSDM) (Baggeroer et. al. 1993) and is defined as such to make MFP independent of the source waveform. The asterisk in (1) and (2) indicates complex conjugation, and G is the calculated Green's function of the (known) environment for a source transmitting at x_t to a receiver at x_j . When defined this way, the ambiguity surface, B_c , is a positive, real, and bounded between 0 and 1, with 1 indicating a perfect match between the measured and calculated fields. Mismatch arises in (1) when $P_j(\omega)$ and $w_j(x_s, \omega)$ differ unintentionally. These differences tend to increase with frequency and source-receiver range. Some of these differences can be compensated by incoherently averaging through the measured signal bandwidth as in (4). Here the signal frequency is assumed to be bounded between Ω_L and Ω_H .

$$B_c(x_t) = \langle B_c(x_t, \omega) \rangle_\omega = \frac{1}{\Omega_H - \Omega_L} \int_{\Omega_L}^{\Omega_H} B_c(x_t, \omega) d\omega \quad (4)$$

Frequency difference techniques, including FDSL, rely on analysing the CSDM of the frequency-difference autoprodut defined in (5) that is measured along the array, and correlating it to a weight vector that matches the physics of the autoprodut.

$$R_{ij}^{AP}(\Delta\omega) = \frac{\langle AP_i^*(\omega, \Delta\omega) AP_j(\omega, \Delta\omega) \rangle_\omega}{\sum_i |\langle AP_i(\omega, \Delta\omega) \rangle_\omega|^2} \quad (5)$$

$$AP_j(\omega, \Delta\omega) = P_j^*(\omega - 0.5\Delta\omega) P_j(\omega + 0.5\Delta\omega) \quad (6)$$

$$w_j(x_t, \Delta\omega) = |G_{modes}(\Delta\omega, x_t, x_j)| \arg(\sum_i |A_i|^2 \exp(i\Delta\omega\tau_i)) \quad (7)$$

$$B_\Delta(x_t, \Delta\omega) = \sum_{i,j} w_i(x_t, \Delta\omega) R_{ij}^{AP}(\Delta\omega) w_j^*(x_t, \Delta\omega) \quad (8)$$

This processing is done by first taking a single sample of the autoprodut, as in (6), where the complex field values measured on one receiver are multiplied to form an autoprodut sample. This sample is then used to compute an autoprodut CSDM, and all samples available in the measured signal bandwidth are averaged and normalized to produce the final CSDM in (5). This CSDM is then cross correlated with the weight vector defined in (7). In (7), the amplitude of the weight vector is calculated using KRAKEN, a normal mode code, (Porter 1987), while its phase is derived from a ray code, Bellhop (Porter 1992). The amplitude follows that of FDMFP (Worthmann 2015), but the phase is derived from considerations of (6) when the measured field is well described as a sum of ray-path contribution with amplitude A_i and arrival times τ_i . The utility of the phase correction employed here is to remove the phase induced on a ray path which has been reflected by a barrier (Kinsler et. al. 2000) or which has passed through a caustic (Jensen et. al. 2011), as such phase corrections are absent from the measured autoprodut (Worthmann and Dowling 2018). Such processing is possible because the user has full control over how the weight vector is calculated in any MFP scheme.

3. EXPERIMENTAL SETUP & RESULTS

The experimental data used in this study was measured during the 2010-2011 Philippine Sea Experiment (PhilSea10) (Worcester et. al 2013). This was an underwater oceanographic

experiment, and the utility of the dataset for source localization research was unexpected. PhilSea10 included the collection of thousands of transmissions that came from a variety of sources. This study explores the first 120 pings (nominally the first 100 pings plus several others for snapshot averaging purposes) measured from the second closest source positioned 210 km downrange from the receiving array. The dataset used was provided to the authors by P. Worcester and M. Dzieciuch, lead scientists on the experiment, as matched-filtered time series for each hydrophone. This matched-filtering process technically requires knowledge of the source waveform, but it is here used only to achieve high SNR. All signal waveforms are scrambled across frequency by applying a random phase to each frequency bin to prevent source waveform information from reaching the signal processing steps. Additionally, the experimentalists also provided an acoustic sound speed profile measured near the receiving array, as well as nominal receiver positions for 149 elements in the receiving array. All calculations were done using this given information without alteration.

Based on this experimental geometry, the performance of conventional MFP and FDSL for both simulated and measured signals was calculated. In simulation, the pressure fields at the array were calculated using Bellhop. For MFP, 21 individual field samples ($f = 200$ Hz, 205 Hz, ..., 300 Hz) from the measured bandwidth were used to construct the ambiguity surface. For FDSL, five difference frequency samples ($\Delta f = 1$ Hz, 1.25 Hz, ..., 2 Hz) were used to construct the ambiguity surface. Fig. 1 shows sample ambiguity surfaces calculated using measured field values for MFP and FDSL. The performance was also calculated for simulated fields, with results being similar to the results given in Fig. 2. In simulation, both

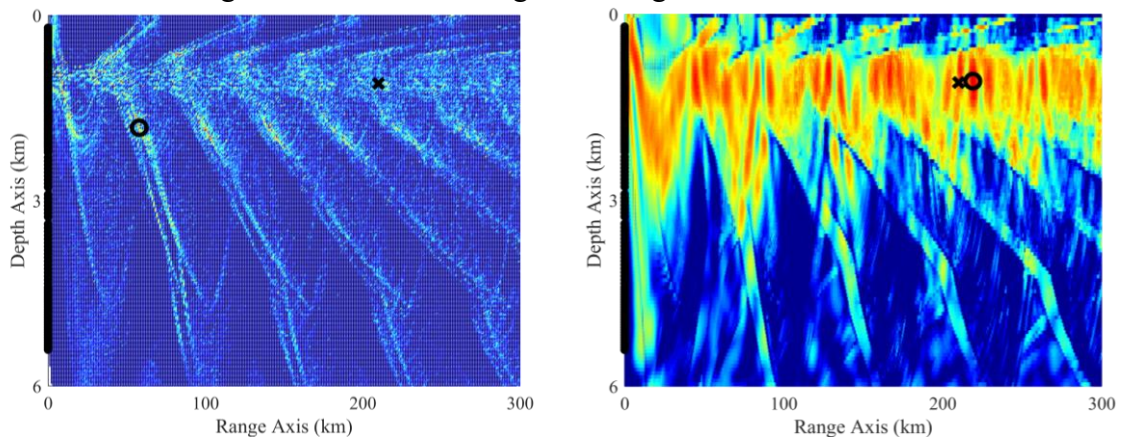


Figure 1: Ambiguity surfaces calculated applying (a) Bartlett MFP, and (b) FDSL to the first valid measurement of the given source during the PhilSea10 exercise.

MFP and FDSL successfully localize the relevant sources. However, in measurement, only FDSL successfully localizes the given sources within $\pm 5\%$ in range and depth. It is worth noting that FDSL shows approximately an 8 km range bias. This range error is seen in all localization results, and could possibly be corrected by taking into account bathymetric variations in the range-depth plane defined by the source and the vertical receiving array.

To demonstrate the robustness of FDSL to environmental mismatch, both types of processing were performed on the first 100 measured transmissions. The source localization results for both algorithms are shown in Fig. 2, along with a nominal localization success boundary that is an ellipse with axes defined by $\pm 5\%$ of the overall search range and depth (± 15 km and ± 300 m, respectively). These bounds are chosen to be reasonable and to indicate that the overall results are not obtained by chance. Initially, 97% of the trials are found to be successful for FDSL and 0% for MFP. Therefore, one final elementary signal processing step, snapshot averaging, was taken. Snapshot averaging is here taken to mean that ambiguity surfaces from successive pings were averaged. With two snapshot averaging, 100% localization success is achieved for FDSL. The localization performance of MFP did not improve for any amount of snapshot averaging (up to 20 snapshots).

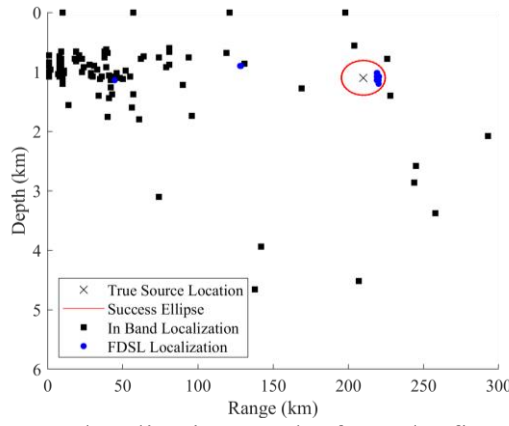


Figure 2: Scatter plot of source localization results from the first 100 pings transmitted by a source 210 km from the vertical receiving array during the PhilSea10 experiment. Conventional MFP does not localize the source. FDSL successfully localizes the source 97 times.

Given these localization results, the robustness of both conventional MFP and FDSL to elevated noise levels was tested. The noise level was varied here by adding either simulated or measured ocean noise. The simulated noise was created in the time domain by generating random numbers according to normal distributions with zero mean and unit standard deviation. This simulated time series was then Fourier transformed to place it into the frequency domain. The measured noise time series was collected during the experiment immediately before the measured signal was received. From here, either noise sample was multiplied by α according to (9) in order to give the desired SNR. This definition of SNR,

$$\text{SNR}(\alpha) = 10(\log_{10}(\sum_i |P_i(\omega)|^2) - \log_{10}(\sum_i |\alpha N_i(\omega)|^2)) \quad (9)$$

is standard (Jensen et. al. 2011). The simulated performance of conventional MFP and FDSL in the presence of elevated levels of simulated noise is shown in Fig. 3. In addition to this, the

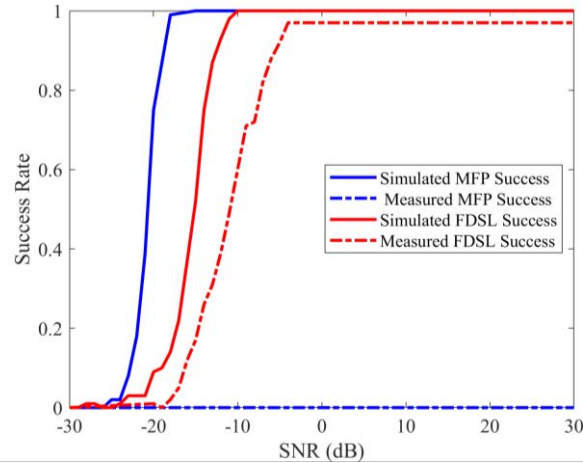


Figure 3: Noise Rejection capabilities of simulated and measured MFP and FDSL for $-30 < \text{SNR} < 30$. Simulations of both are conducted by using Bellhop to compute a forward field, and simulated noise is added to this field at a given SNR. Measurements of both are computed by adding measured noise to the given measured signal.

measured performance of MFP and FDSL in the presence of measured noise is also shown in Fig. 3. Here, success is determined by the percentage of successful localizations based on the success criterion defined in Fig. 2. The simulated results show that MFP has the best noise rejection capability. Despite this, MFP fails to successfully localize a source at any SNR using measured signals. FDSL, while not as robust to simulated noise as is MFP, is capable of

localizing sources down to SNRs of -8 dB or so in the presence of both simulated and measured noise.

4. SUMMARY AND CONCLUSIONS

Frequency-difference source localization (FDSL) is a new below-band technique for source localization in imperfectly known deep ocean environments that is akin to conventional matched field processing (MFP). FDSL successfully localizes a source positioned 210 km downrange from a vertical receiving array in the Philippine Sea using both simulated and measured data. In the chosen difference-frequency range, the performance of FDSL is robust to measured-field-to-calculated-field mismatch that is ubiquitous in long range acoustic propagation in the deep ocean. The noise rejection capabilities of both algorithms were also explored. Using simulated data, MFP rejects noise down to SNRs near -20 dB without mismatch, but fails to localize the source (at all SNRs) using PhilSea10 experimental data. However, using both simulated and experimental data, FDSL is able to successfully localize the source down to SNRs near -8 dB. Approaches that allow FDSL to inherit the greater noise rejection capabilities of MFP are now being explored.

REFERENCES

- [1] **Dowling, D.R. and K. Sabra**, Acoustic Remote Sensing, *Ann. Rev. Fluid Mech.* 47, pp. 221-243, 2015.
- [2] **Bucker**, Use of calculated sound fields and matched-field detection to locate sound sources in shallow water. *J. Acoust. Soc. Am.* 59, pp. 368, 1976.
- [3] **Debever, C, and W.A. Kuperman**, Robust matched-field processing using a coherent broadband white noise constraint processor, *J. Acoust. Soc. Am.* 122, pp. 1979-1986, 2007.
- [4] **Baggeroer, A.B., W.A. Kuperman, and P.N. Mikhalevsky**. An overview of matched field methods in ocean acoustics. *IEEE J. Ocean Eng.* 18, pp. 3018-3029, 1993.
- [5] **Worthmann, B.M., H.C. Song, and D.R. Dowling**, High frequency source localization in a shallow ocean using frequency-difference matched field processing. *J. Acoust. Soc. Am.* 138, pp 3549, 2015.
- [6] **Worthmann, B.M., H.C. Song, and D.R. Dowling**, Adaptive frequency-difference matched field processing for high frequency source localization in a noisy shallow ocean. *J. Acoust. Soc. Am.* 141, pp. 543-556, 2017.
- [7] **Worcester, P.F., M.A. Dzieciuch, J.A. Mercer, R.K. Andrew, B.D. Dushaw, A.B. Baggeroer, K.D. Heaney, G.L. D'Spain, J.A. Colosi, R.A. Stephen, J.N. Kemp, B.M. Howe, L.J. van Uffelen, and K.E. Wage**. The North Pacific Acoustic Laboratory deep-water acoustic propagation experiments in the Philippine Sea, *J. Acoust. Soc. Am.*, 134(4), pp. 3359-3375, 2013.
- [8] **Jensen, F.B., W.A. Kuperman, M.B. Porter, and H. Schmidt**. *Computational Ocean Acoustics*, 2nd Ed., AIP, pp. 705-722, 2011.
- [9] **Porter, M.B. and H.P. Bucker**. Gaussian beam tracing for computing ocean acoustic fields. *J. Acoust. Soc. Am.* 82, pp. 1349-1359, 1987.
- [10] **Porter, M.** The KRAKEN normal mode program. Defense Technical Information Center (DTIC).
- [11] **Kinsler, L.E., A.R. Frey, A.B. Coppens, J.V. Sanders**, *Fundamentals of Acoustics*, 4th Ed., J. Wiley & Sons, 2000.
- [12] **Worthmann, B.M. and D.R. Dowling**. The frequency-difference and frequency-sum acoustic-field autoproductions. *J. Acoust. Soc. Am.* 141, pp 4579, 2017.